Synthesis, Structure, and Magnetic and Redox Properties of Linear Bis-Dinuclear Complexes Afforded by Schiff Base Ligands Containing Catecholate and Pyridine or Imidazole Groups

ARTICLE *in* INORGANIC CHEMISTRY · DECEMBER 1997

Impact Factor: 4.76 · DOI: 10.1021/ic9703538

7 AUTHORS, INCLUDING:

Rajeev Chikate
Abasaheb Garware College
50 PUBLICATIONS **1,269** CITATIONS
SEE PROFILE

Subhash Padhye
Abeda Inamdar Senior College
237 PUBLICATIONS **5,817** CITATIONS
SEE PROFILE

Synthesis, Structure, and Magnetic and Redox Properties of Linear Bis-Dinuclear Complexes Afforded by Schiff Base Ligands Containing Catecholate and Pyridine or Imidazole Groups

Sylvie Theil,[†] Ratnamala Yerande,[‡] Rajeev Chikate,[‡] Françoise Dahan,[†] Azzedine Bousseksou,[†] Subhash Padhye,*[,‡] and Jean-Pierre Tuchagues*[,†]

Department of Chemistry, University of Poona, Pune 411007, India, and Laboratoire de Chimie de Coordination du CNRS, UP 8241 liée par conventions à l'Université Paul Sabatier et à l'Institut National Polytechnique, 205 route de Narbonne, 31077 Toulouse Cedex, France

Received March 27, 1997[⊗]

Three complexes, $[Mn^{II}_2L^1(CH_3CO_2)_2(CH_3OH)]_2$ (**1**), $(Mn^{II}_2L^2(CH_3CO_2)_2\ (CH_3OH))_2$ (**2**), and $(Mn^{II}_2HL^3(CH_3CO_2)_2(CH_3OH))_2$ (**3**), wherein H_2L^1 = 3-[(((2′-pyridyl)methyl)imino)methyl]benzene-1,2-diol, H_2L^2 = 3-[((2-(2′-pyridyl)ethyl)imino)methyl]benzene-1,2-diol, and H_3L^3 = 3-[((2-(4′-imidazolyl)ethyl)imino)methyl]benzene-1,2-diol, have been synthesized and studied. **1** crystallizes in the monoclinic system, space group $P2_1/c$, $Z = 2$, $a = 11.396(1)$ Å, $b = 18.583(2)$ Å, $c = 9.888(1)$ Å, and $\beta = 103.51(1)°$. The structure was solved by direct methods and refined to conventional agreement indices $R = 0.028$ and $R_w = 0.029$. The molecular structure of **1** consists of discrete $[Mn^{II}_2L^1(CH_3CO_2)_2(CH_3OH)]_2$ molecules. **1** is a chainlike bis-dinuclear Mn(II) complex involving an unprecedented arrangement of pentacoordinated (N_2O_3) and hexacoordinated (O_6) manganese ions as the outer and inner pairs of metal centers, respectively. The different Mn···Mn distances result from significant differences in bridging moieties, two catecholato bridges for the shortest distance between inner manganese ions, and one catecholato and two acetato bridges for the longer distances between inner and outer manganese ions. The symmetry of the N_2O_3 donor set around the outer Mn(1) is close to a trigonal bipyramid while the O_6 ligand environment of the inner Mn(2) can be described as a rhombically distorted octahedron. The synthesis, IR, EPR, and magnetic susceptibility of **1**−**3** suggest a similar bis-dinuclear structure for all three complexes. Variable-temperature magnetic susceptibility studies establish the presence of antiferromagnetic exchange interactions between Mn(II) centers of **1**−**3** with predominence of the interactions between inner and outer metal ions (−3.4 to −5 cm^{-1}) over the interaction between inner manganese ions (−0.5 to 0.5 cm^{-1}). EPR spectroscopy indicates that the bis-dinuclear arrangement of complexes **1**−**3** is retained in aprotic solvents. As shown by EPR, O_2 oxidation leads to the release of the constitutive Mn(II) dinuclear units, prior to formation of mononuclear Mn(II) and finally Mn(III) species. Observation of two irreversible two-electron oxidation waves in the CV profiles of **1**−**3** is consistent with a similar splitting of the bis-dinuclear complex molecules induced by electrochemical oxidation. These studies suggest that complexes resulting from the reaction of manganese with the fully oxidized form of such electroactive ligands may afford interesting new higher oxidation-state polynuclear Mn species.

Introduction

In the expanding field of manganese polynuclear complexes, tetranuclear assemblies have received much attention during the past 15 years due to the involvement of four interacting manganese ions with variable oxidation states in the oxygen-evolving complex (OEC) of photosystem 2.[1] Thus, numerous tetranuclear complexes have been prepared and studied with overall oxidation state for the four manganese ions comprised between +8 and +16 and a variety of nitrogen- and/or oxygen-

* To whom correspondence should be addressed. Fax: (33) 561 553003. E-mail: tuchague@lcctoul.lcc-toulouse.fr.

[†] Laboratoire de Chimie de Coordination.

[‡] University of Poona.

[⊗] Abstract published in *Advance ACS Abstracts,* December 1, 1997.

(1) See for example: (a) *Manganese Redox Enzymes;* Pecoraro, V. L., Ed.; VCH Publishers: New York, 1992. (b) Debus, R. J. *Biochim. Biophys. Acta* **1992**, *1102*, 269. (c) Rutherford, A. W.; Zimmerman, J.-L.; Boussac, A. In *The Photosystems: Structure, Function and Molecular Biology*; Barber, J., Ed.; Elsevier Science Publishers: New York, 1992; Chapter 5.

(2) (a) Wieghardt, K.; Bossek, U.; Gebert, W. *Angew. Chem., Int. Ed. Engl.* **1983**, *4*, 328. (b) Costa, T.; Dorfman, J. R.; Hagen, K. S.; Holm, R. H. *Inorg. Chem.* **1983**, *22*, 4091. (c) Hagen, K. S.; Westmoreland, T. D.; Scott, M. J.; Armstrong, W. H. *J. Am. Chem. Soc.* **1989**, *111*, 1907. (d) Beagley, B.; McAuliffe, C. A.; MacRory, P. P.; Ndifon, P. T.; Pritchard, R. G. *J. Chem. Soc., Chem. Commun*. **1990**, 309. (e) Beagley, B.; Mackie, A. G.; Matear, P. P.; McAuliffe, C. A.; Ndifon, P. T.; Pritchard, R. G. *J. Chem. Soc., Chem. Commun*. **1992**, 1301. (f) Gallo, E.; Solari, E.; De Angelis, S.; Floriani, C.; Re, N.; Chiesi-Villa, A.; Rizzoli, C. *J. Am. Chem. Soc.* **1993**, *115*, 9850. (g) Stephan, H. O.; Griesar, K.; Haase, W.; Henkel, G. *Z. Naturforsch.* **1994**, *49b*, 1620.

(3) (a) Smit, J. J.; Nap, G. M.; De Jongh, L. J.; Van Ooijen, J. A. C.; Reedijk, J. *Physica* **1979**, *97B*, 365. (b) Horn, E.; Snow, M. R.; Zeleny, P. C. *Aust. J. Chem.* **1980**, *33*, 1659. (c) Ten Hoedt, R. W. M.; Reedijk, J. *Inorg. Chim. Acta* **1981**, *51*, 23. (d) Lynch, M. W.; Hendrickson, D. N.; Fitzgerald, B. J.; Pierpont, C. G. *J. Am. Chem. Soc.* **1981**, *103*, 3961. (e) Lynch, M. W.; Hendrickson, D. N.; Fitzgerald, B. J.; Pierpont, C. G. *J. Am. Chem. Soc.* **1984**, *106*, 2041. (f) McKee, V.; Shepard, W. B. *J. Chem. Soc., Chem. Commun.* **1985**, 158. (g) Brooker, S.; McKee, V.; Shepard, W. B.; Pannell, L. K. *J. Chem. Soc., Dalton Trans.* **1987**, 2555. (h) Bashkin, J. S.; Chang, H. R.; Streib, W. E.; Huffman, J. C.; Hendrickson, D. N.; Christou, G. *J. Am. Chem. Soc.* **1987**, *109*, 6502. (i) Li, Q.; Vincent, J. B.; Libby, E.; Chang, H. R.; Huffman, J. C.; Boyd, W.; Christou, G.; Hendrickson, D. N. *Angew. Chem., Int. Ed. Engl.* **1988**, *27*, 1731. (j) Hendrickson, D. N.; Christou, G.; Schmitt, E. A.; Libby, E.; Bashkin, J. S.; Wang, S.; Tsai, H.; Vincent, J. B.; Boyd, W.; Huffman, J. C.; Folting, K.; Li, Q.; Streib, W. E. *J. Am. Chem. Soc.* **1992**, *114*, 2455. (k) Wang, S.; Tsai, H.; Streib, W. E.; Christou, G.; Hendrickson, D. N. *J. Chem. Soc., Chem. Commun*. **1992**, 1427. (l) Gedye, C.; Harding, C.; McKee, V., Nelson, J.; Patterson, J. *J. Chem. Soc., Chem. Commun*. **1992**, 392. (m) Shoner, S. C.; Power, P. P. *Inorg. Chem.* **1992**, *31*, 1001. (o) Taft, K. L.; Caneschi, A.; Pence, L. E.; Delfs, C. D.; Papaefthymiou, G. C.; Lippard, S. J. *J. Am. Chem. Soc.* **1993**, *115*, 11753. (n) Wang, S.; Tsai, H.; Hagen, K. S.; Hendrickson, D. N.; Christou, G. *J. Am. Chem. Soc.* **1994**, *116*, 8376.

S0020-1669(97)00353-4 CCC: $14.00

containing ligands affording diverse topological arrangements of the four manganeses. They are usually described with reference to known structures or to the overall shape of the complex like adamantane (tetrahedral),[2] cubane,[3] butterfly shaped,[4] and bis-dinuclear with either arrangement of the two dinuclear units in two superposed planes[5] or in the same plane leading to approximately linear or chainlike clusters.[6] However, owing to the large variety of tetranuclear manganese assemblies, a number of them do not pertain to previously described arrangements.[7]

The tetranuclear manganese complexes including catecholate or related ligands have cubane structures involving four Mn(II) ions.[3d,e,m] On the other hand, catechol-based ligands with N_2O_2 donor sets resulting from the Schiff base condensation of 2,3-dihydroxybenzaldehyde with 2-H_2NR-pyridine (R = methyl, ethyl) allow formation of tetranuclear copper(II) complexes with either bis-dinuclear[8] or cubane[8b] structures depending on R and on the bridging ability of the anions. These results prompted us to explore the ability of such ligands to afford tetranuclear manganese complexes of the bis-dinuclear type.

In this contribution, we describe the preparation and IR, EPR, variable-temperature magnetic susceptibility, and electrochemical and O_2 oxidation results for $[Mn^{II}_2L^1(CH_3CO_2)_2(CH_3OH)]_2$ (**1**), $(Mn^{II}_2L^2(CH_3CO_2)_2(CH_3OH))_2$ (**2**), and $(Mn^{II}_2HL^3(CH_3CO_2)_2(CH_3OH))_2$ (**3**) (H_2L^1 = 3-[(((2′-pyridyl)methyl)imino)methyl]benzene-1,2-diol, H_2L^2 = 3-[((2-(2′-pyridyl)ethyl)imino)methyl]benzene-1,2-diol, and H_3L^3 = 3-[((2′-(4′-imidazolyl)ethyl)imino)methyl]benzene-1,2-diol (Figure 1)). H_3L^3 is a new potentially electroactive ligand including both a catechol and an imidazole moiety which is an interesting situation with regard to the possibility of an histidine imidazole oxidation in the S_3 state of Kok's cycle.[9] The X-ray crystal structure of **1** has been determined providing evidence for the chainlike arrangement of the two dinuclear units forming the novel Mn^{II}_4 complexes including these catecholate ligands.

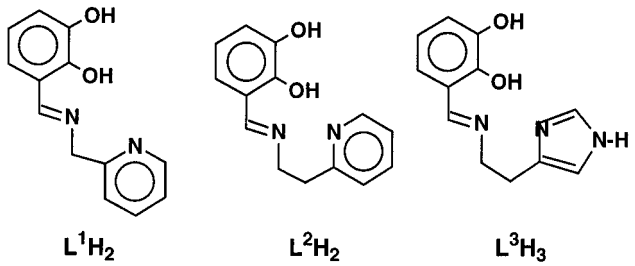

Figure 1. Schematic representation of the H_2L^1, H_2L^2, and H_3L^3 ligands.

Experimental Section

Materials. 2,3-Dihydroxybenzaldehyde (Fluka), 2-(aminomethyl)pyridine (Aldrich), 2-(2-aminoethyl)pyridine (Janssen), histamine dihydrochloride (Fluka), and manganese(II) acetate tetrahydrate (Alfa) were used as purchased. High-grade solvents used for the synthesis of complexes were degassed under vacuum prior to use.

Ligands. 3-[(((2′-Pyridyl)methyl)imino)methyl]benzene-1,2-diol (H_2L^1) and 3-[((2-(2′-Pyridyl)ethyl)imino)methyl]benzene-1,2-diol (H_2L^2). Both Schiff bases were prepared according to the method reported by Gojon et al.,[8b] *i.e.* condensation of 2,3-dihydroxybenzaldehyde (0.69 g, 5×10^{-3} mol) with 2-(aminomethyl)pyridine (0.55 g, 5×10^{-3} mol) and 2-(2-aminoethyl)pyridine (0.62 g, 5×10^{-3} mol) for H_2L^1 and H_2L^2, respectively. H_2L^1: Yellow powder; yield 0.97 g (85.5%). Anal. Calcd for $C_{13}H_{12}N_2O_2$: C, 68.39; H, 5.30; N, 12.27. Found: C, 68.25; H, 5.72; N, 12.76. H_2L^2: Orange powder; yield 1.16 g (96%). Anal. Calcd for $C_{14}H_{14}N_2O_2$: C, 69.40; H, 5.82; N, 11.56. Found: C, 69.16; H, 6.45; N, 11.79.

3-[((2-(4′-Imidazolyl)ethyl)imino)methyl]benzene-1,2-diol (H_3L^3). Histamine dihydrochloride (1.15 g, 5×10^{-3} mol) was slowly added to a stirred solution of sodium ethanolate (10^{-2} mol in 20 mL of absolute ethanol). After the reaction mixture was stirred for 1 h, the NaCl precipitate was filtered off. 2,3-Dihydroxybenzaldehyde (0.69 g, 5×10^{-3} mol) was then slowly added to the histamine solution, and the reaction mixture was stirred for an additional 1 h during which the 2,3-dihydroxybenzaldehyde dissolved completely and the colorless solution turned to deep yellow. Concentration of the ethanolic solution to 10 mL afforded H_3L^3 as a fine orange powder collected by filtration and dried overnight under vacuum. Yield: 0.77 g (67.5%). Anal. Calcd for $C_{12}H_{13}N_3O_2$: C, 62.31; H, 5.67; N, 18.17. Found: C, 62.44; H, 5.90; N, 18.17.

Complexes. Complexes **1**−**3** were prepared under an atmosphere of purified nitrogen by using standard Schlenk techniques, dried under vacuum, and stored in an inert-atmosphere box (Vacuum Atmospheres H.E.43.2) equiped with a Dri-Train (Jahan EVAC 7). In a typical reaction, a carefully degassed solution of $Mn(OAc)_2 \cdot 4H_2O$ (10^{-2} mol) in methanol (10 mL) was slowly added to the ligand suspension under stirring (5×10^{-3} mol in 40 mL of absolute ethanol) which resulted in complete dissolving of the ligand. The complex precipitated as an abundant yellow powder within 1−3 h. The slurry was warmed to 50 °C for 1 h under stirring (except for **3**), cooled at room temperature, collected by filtration, washed with MeOH, and dried overnight under vacuum.

$[Mn_2L^1(CH_3CO_2)_2(CH_3OH)]_2$ (**1**): Yield 1.99 g (82%). Anal. Calcd for $Mn_2C_{18}H_{20}N_2O_7$: C, 44.47; H, 4.15; N, 5.76; Mn, 22.60. Found: C, 45.24; H, 4.30; N, 5.79; Mn, 22.52. $(Mn_2L^2(CH_3CO_2)_2(CH_3OH))_2$ (**2**): Yield 1.7 g (68%). Anal. Calcd for $Mn_2C_{19}H_{22}N_2O_7$: C, 45.61; H, 4.43; N, 5.60; Mn, 21.96. Found: C, 45.02; H, 4.27; N, 5.48; Mn,

(4) (a) Vincent, J. B.; Christmas, C.; Huffman, J. C.; Christou, G.; Chang, H. R.; Hendrickson, D. N. *J. Chem. Soc., Chem. Commun*. **1987**, 236. (b) Christmas, C.; Vincent, J. B.; Huffman J. C.; Christou, G.; Chang, H. R.; Hendrickson, D. N. *J. Chem. Soc., Chem. Commun*. **1987**, 1303. (c) Kulawiec, R. J.; Crabtree, R. H.; Brudvig, G. W.; Schulte, G. K. *Inorg. Chem*. **1988**, *27*, 1309. (d) Chandra, S. K.; Chakrovorty, A. *Inorg. Chem.* **1991**, *30*, 3795. (e) Libby, E.; McCusker, J. K.; Schmitt, E. A.; Folting, K.; Hendrickson, D. N.; Christou, G. *Inorg. Chem.* **1991**, *30*, 3486. (f) Wang, S.; Huffman J. C.; Folting, K.; Streib, W. E.; Lobkovsky, E. B.; Christou, G. *Inorg. Chem.* **1991**, *30*, 3486; *Angew. Chem., Int. Ed. Engl.* **1991**, *30*, 1672. (g) Bouwman, E.; Bolcar, M. A.; Libby, E.; Huffman J. C.; Folting, K.; Christou, G. *Inorg. Chem.* **1992**, *31*, 5185.

(5) (a) Luneau, D.; Savariault, J.-M.; Cassoux, P.; Tuchagues, J.-P. *J. Chem. Soc., Dalton Trans.* **1988**, 1225. (b) Brooker, S.; McKee, V. *J. Chem. Soc., Chem. Commun*. **1989**, 619. (c) Stibrany, R. T.; Gorun, S. M. *Angew. Chem., Int. Ed. Engl.* **1990**, *29*, 1156. (d) Mikuriya, M.; Yamato, Y.; Tokii, T. *Chem. Lett.* **1991**, 1429. (e) Chan, M. K.; Armstrong, W. H. *J. Am. Chem. Soc.* **1991**, *113*, 5055. (f) Susuki, M.; Hayashi, Y.; Munezawa, K.; Suenaga, M.; Senda, H.; Uehara, A. *Chem. Lett.* **1991**, 1929. (g) Mikuriya, M.; Yamato, Y.; Tokii, T. *Bull. Chem. Soc. Jpn.* **1992**, *65*, 2624.

(6) (a) Chan, M. K.; Armstrong, W. H. *J. Am. Chem. Soc.* **1989**, *111*, 9121. (b) Susuki, M.; Sugisawa, T.; Senda, H.; Oshio, H.; Uehara, A. *Chem. Lett.* **1989**, 1091. (c) Susuki, M.; Senda, H.; Suenaga, M.; Sugisawa, T.; Uehara, A. *Chem. Lett.* **1990**, 923. (d) Chan, M. K.; Armstrong, W. H. *J. Am. Chem. Soc.* **1990**, *112*, 4985. (e) Sakiyama, H.; Tokuyama, K.; Matsumura, Y.; Okawa, H. *J. Chem. Soc., Dalton Trans.* **1993**, 2329. (f) Jeffery, J. C.; Thornton, P.; Ward, M. D. *Inorg.Chem.* **1994**, *33*, 3612. (g) Philouze, C.; Blondin, G.; Girerd, J.-J.; Guilhem, J.; Pascard, C.; Lexa, D. *J. Am. Chem. Soc.* **1994**, *116*, 8557.

(7) See for example: (a) McKee, V.; Tandon, S. S. *J. Chem. Soc., Chem. Commun*. **1988**, 1334. (b) Saalfrank, R. W.; Stark, A.; Bremer, M.; Hummel, H.-U. *Angew. Chem., Int. Ed. Engl.* **1990**, *29*, 311. (c) Jiang, Z.-H.; Ma, S.-L.; Liao, D.-Z.; Yan, S.-P.; Wang, G.-L.; Yao, X.-K.; Wang, R.-J. *J. Chem. Soc., Chem. Commun*. **1993**, 745. (d) Gultneh, Y.; Ahvazi, B.; Raza Khan, A.; Butcher, R. J.; Tuchagues, J.-P. *Inorg. Chem.* **1995**, *34*, 3633.

(8) (a) Gojon, E.; Greaves, S. J.; Latour, J. M.; Povey, D. C.; Smith, G. W. *Inorg. Chem.* **1987**, *26*, 1457. (b) Gojon, E.; Latour, J. M.; Greaves, S. J.; Povey, D. C.; Ramdas, V.; Smith, G. W. *J. Chem. Soc., Dalton Trans.* **1990**, 2043.

(9) (a) Boussac, A.; Zimmermann, J. L.; Rutherford, A. W. *Biochemistry* **1989**, *28*, 8984. (b) Boussac, A.; Zimmermann, J. L.; Rutherford, A. W.; Lavergne, J. *Nature* **1990**, *347*, 303. (c) Boussac, A.; Zimmermann, J. L.; Rutherford, A. W. *FEBS Lett.* **1990**, *277*, 69. (d) Rutherford, A. W.; Boussac, A.; Zimmermann, J. L. *New J. Chem.* **1991**, *15*, 491.

21.44. $(Mn_2HL^3(CH_3CO_2)_2(CH_3OH))_2$ (**3**): Yield 0.97 g (40%). Anal. Calcd for $Mn_2C_{17}H_{21}N_3O_7$: C, 41.74; H, 4.33; N, 8.59; Mn, 22.46. Found: C, 42.31; H, 4.38; N, 8.43; Mn, 22.3.

Orange-red single crystals of **1** suitable for X-ray diffraction studies were obtained by slow interdiffusion (2 months) between a deoxygenated methanolic solution (45 mL) of $Mn^{II}(CH_3CO_2)_2{\cdot}4H_2O$ (2×10^{-4} mol) and a deoxygenated methanolic solution (45 mL) of H_2L^1 (10^{-4} mol).

Physical Mesurements. Elemental analyses were carried out at the Laboratoire de Chimie de Coordination Microanalytical Laboratory in Toulouse, France, for C, H, and N and at the Service Central de Microanalyses du CNRS in Vernaison, France, for Mn. IR spectra were recorded on a Perkin-Elmer 983 spectrophotometer coupled with a Perkin-Elmer infrared data station. Samples were run as CsBr pellets prepared under nitrogen in the drybox.

Variable-temperature magnetic susceptiblity data were obtained on powdered polycrystalline samples with a Quantum Design MPMS SQUID susceptometer. Diamagnetic corrections were applied by using Pascal's constants. Least-squares computer fittings of the magnetic susceptibility data were accomplished with an adapted version of the function-minimization program STEPT.[10]

X-band EPR spectra were obtained on a Bruker ESP 300 E spectrometer with magnetic field modulation at 100 kHz. The microwave frequency was measured with a Racal-Dana frequency meter, and the magnetic field was measured with a Bruker NMR probe gaussmeter. A Bruker liquid-nitrogen cryostat was used for measurements between 300 and 90 K. Powdered and DMF/toluene or $C_2H_4Cl_2$/toluene samples were loaded in 4 mm cyclindrical quartz tubes in the drybox and then degassed and sealed under vacuum.

Cyclic voltammograms ($0.1-20$ V s^{-1}) were obtained with a three-electrode cell comprised of a platinum, gold, or glassy carbon working electrode, a Pt wire counter electrode, and a SCE reference electrode. Linear voltammograms (5 mV s^{-1}) were performed with a platinum rotating disk (10^3 rpm).

X-ray Crystal Structure Determination of 1. An orange-red square plate ($0.50 \times 0.50 \times 0.125$ mm) was sealed on a glass fiber and mounted on an Enraf-Nonius CAD 4 diffractometer. A total of 4200 reflections (3974 unique) with $2\theta \leq 52°$ were collected at 20 °C using Mo Kα radiation with a graphite monochromator ($\lambda = 0.710\ 73$ Å). The crystal of $[Mn_2L^1(CH_3CO_2)_2\ (CH_3OH)]_2$ belongs to the monoclinic system, and its space group was assigned as $P2_1/c$ from extinctions $h0l$, $l = 2n + 1$, and $0k0$, $k = 2n + 1$. The crystal quality was monitored by scanning three standard reflections every 2 h. No significant variation was observed during the data collection. After corrections for Lorentz and polarization effects,[11] an empirical absorption correction was applied.[12]

Structure Solution and Refinement. The structure was solved by using direct methods[13] and refined by full-matrix least squares.[14] All non-hydrogen atoms were refined anisotropically. Hydrogen atoms were found on a difference Fourier synthesis. The H(O7) hydrogen atom of the methanol molecule was refined while the others were included in calculations with a constrained geometry (C−H = 0.97 Å). The atomic scattering factors and anomalous dispersion terms were taken from the standard compilation.[15] The final refinement cycle converged to $R(F_o) = 0.028$ and $R_w = 0.029$ with unit weights. The goodness of fit was $s = 1.100$ with 2745 reflections having $F_o^2 > 6\sigma(F_o)$ and 265 variable parameters.

All calculations were performed on a MicroVAX 3400 computer using the programs MOLEN,[11] SHELXS-86,[13] SHELX 76,[14] and ORTEP.[16] The $[Mn_2L^1(CH_3CO_2)_2(CH_3OH)]_2$ complex molecule is shown in Figure 2 with atom numbering. The crystallographic data are summarized in Table 1. Final fractional atomic coordinates with their estimated standard deviations and selected bond lengths and angles are given in Tables 2 and 3, respectively.

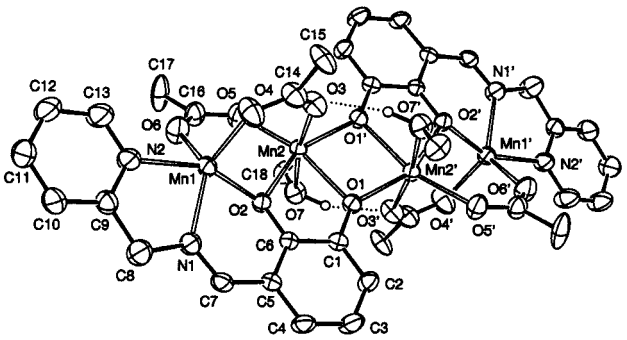

Figure 2. ORTEP view of the $[Mn_2L^1(CH_3CO_2)_2(CH_3OH)]_2$ molecule (**1**) with atom numbering.

Table 1. Crystallographic Data for $[Mn_2L^1(CH_3CO_2)_2\ (CH_3OH)]_2$ (**1**)

chem formula: $Mn_4C_{36}H_{40}N_4O_{14}$	fw: 972.48
space group: $P2_1/c$ (No. 14)	$T = 20$ °C
$a = 11.396(1)$ Å	
$b = 18.583(2)$ Å	$\beta = 103.51(1)°$
$c = 9.888(1)$ Å	
$V = 2036.1(7)$ Å^3	$\lambda = 0.710\ 73$ Å
$\rho_{calc} = 1.586$ g cm^{-3}	μ(Mo Kα) = 12.3 cm^{-1}
$Z = 2$	transm coeff = 0.948−0.999
$R\ (\sum\|\|F_o\| - \|F_c\|\|)/(\sum\|F_o\|) =$ 0.028	$R_w\ ([\sum(\|F_o\| - \|F_c\|)^2/(\sum\|F_o\|)^2]^{1/2}) =$ 0.029

Table 2. Fractional Atomic Coordinates and Isotropic Equivalent Temperature Factors (Å$^2 \times 100$) with ESD's in Parentheses for $[Mn_2L^1(CH_3CO_2)_2(CH_3OH)]_2$ (**1**)

atom	*x/a*	*y/b*	*z/c*	U_{eq}[a]
Mn(1)	0.23733(4)	0.60882(2)	0.10440(5)	3.49(2)
Mn(2)	0.36592(4)	0.52696(2)	0.41241(5)	3.17(2)
O(1)	0.5539(2)	0.5582(1)	0.4599(2)	3.6(1)
O(2)	0.3722(2)	0.6198(1)	0.2820(2)	3.4(1)
O(3)	0.3737(2)	0.4568(1)	0.2329(2)	5.0(1)
O(4)	0.2805(3)	0.5106(1)	0.0365(3)	6.0(2)
O(5)	0.1772(2)	0.5288(1)	0.3958(2)	5.2(1)
O(6)	0.0997(2)	0.5890(1)	0.2017(3)	5.7(2)
O(7)	0.3839(2)	0.5911(1)	0.6216(2)	5.0(1)
N(1)	0.3100(2)	0.7100(2)	0.0445(3)	4.3(2)
N(2)	0.1000(2)	0.6483(2)	−0.0777(3)	4.4(2)
C(1)	0.5791(3)	0.6150(2)	0.3898(3)	3.0(2)
C(2)	0.6937(3)	0.6429(2)	0.4061(3)	3.9(2)
C(3)	0.7150(3)	0.7026(2)	0.3294(4)	4.9(2)
C(4)	0.6230(3)	0.7331(2)	0.2333(3)	4.2(2)
C(5)	0.5051(3)	0.7054(2)	0.2101(3)	3.2(2)
C(6)	0.4818(2)	0.6472(2)	0.2918(3)	2.8(1)
C(7)	0.4161(3)	0.7350(2)	0.0953(3)	3.8(2)
C(8)	0.2365(3)	0.7486(2)	−0.0744(4)	6.4(3)
C(9)	0.1221(3)	0.7094(2)	−0.1385(3)	4.2(2)
C(10)	0.0414(3)	0.7359(2)	−0.2547(4)	5.0(2)
C(11)	−0.0637(3)	0.7003(2)	−0.3077(4)	5.3(2)
C(12)	−0.0888(4)	0.6383(2)	−0.2435(4)	5.9(2)
C(13)	−0.0045(4)	0.6144(2)	−0.1294(4)	6.0(2)
C(14)	0.3404(3)	0.4600(2)	0.1038(4)	5.0(6)
C(15)	0.3745(5)	0.3992(3)	0.0203(5)	10.2(4)
C(16)	0.0924(3)	0.5578(2)	0.3118(4)	4.8(2)
C(17)	−0.0306(4)	0.5578(3)	0.3419(5)	11.3(4)
C(18)	0.3141(4)	0.5747(3)	0.7178(5)	9.7(4)

[a] $U_{eq} = {}^1/_3$ of the trace of the orthogonalized $\mathbf{U}_{ij}$ tensor.

Results and Discussion

Synthesis and Compositional Studies. The analytical results indicate that the reaction of H_2L^1, H_2L^2, and H_3L^3 with

(10) Chandler, J. P. Program 66, Quantum Chemistry Program Exchange, Indiana University, 1973.
(11) Fair, C. K. *MOLEN, Molecular Structure Solution Procedures*; Enraf-Nonius: Delft, The Netherlands, 1990.
(12) North, A. C. T.; Phillips, D. C.; Mathews, F. S. *Acta Crystallogr., Sect. A: Found. Crystallogr.* **1968**, *A24*, 351.
(13) Sheldrick, G. M. *SHELXS-86. Program for Crystal Structure Solution*; University of Göttingen: Göttingen, Germany, 1986.
(14) Sheldrick, G. M. *SHELX 76. Program for Crystal Structure Determination*; University of Cambridge: Cambridge, England, 1976.
(15) *International Tables for X-ray Crystallography*; Kynoch Press: Birmingham, England, 1974; Vol. IV.
(16) Johnson, C. K. *ORTEP, Report ORNL-3794*; Oak Ridge National Laboratory: Oak Ridge, TN, 1965.

Table 3. Selected Interatomic Distances (Å) and Angles (deg) for $[Mn_2L^1(CH_3CO_2)_2(CH_3OH)]_2$ (**1**)[a]

Manganese Environment			
Mn(1)−O(2)	2.056(2)	Mn(2)−O(1)	2.162(2)
Mn(1)−O(4)	2.045(3)	Mn(2)−O(1′)	2.096(2)
Mn(1)−O(6)	2.056(3)	Mn(2)−O(2)	2.165(2)
Mn(1)−N(1)	2.191(3)	Mn(2)−O(3)	2.220(2)
Mn(1)−N(2)	2.216(3)	Mn(2)-O(5)	2.118(2)
Mn(1)···Mn(2)	3.4135(6)	Mn(2)−O(7)	2.354(2)
		Mn(2)···Mn(2′)	3.2970(8)
Mn(1)−O(2)−Mn(2)	107.93(8)	Mn(2)−O(1)−Mn(2′)	101.45(8)
O(2)−Mn(1)−O(4)	100.36(8)	O(1)−Mn(2)−O(1′)	78.55(8)
O(2)−Mn(1)−O(6)	96.76(8)	O(1)−Mn(2)−O(2)	75.32(7)
O(2)−Mn(1)−N(1)	83.79(8)	O(1)−Mn(2)−O(3)	96.22(8)
O(2)−Mn(1)−N(2)	154.99(9)	O(1)−Mn(2)−O(5)	161.59(9)
O(4)−Mn(1)−O(6)	105.2(1)	O(1)−Mn(2)−O(7)	78.17(8)
O(4)−Mn(1)−N(1)	122.8(1)	O(1′)−Mn(2)−O(2)	152.86(7)
O(4)−Mn(1)−N(2)	101.95(9)	O(1′)−Mn(2)−O(3)	86.87(8)
O(6)−Mn(1)−N(1)	131.1(1)	O(1′)−Mn(2)−O(5)	110.51(9)
O(6)−Mn(1)−N(2)	88.2(1)	O(1′)−Mn(2)−O(7)	85.20(8)
N(1)−Mn(1)−N(2)	74.70(9)	O(2)−Mn(2)−O(3)	88.76(8)
O(2)−Mn(2)−O(5)	96.63(8)	O(2)−Mn(2)−O(7)	96.43(8)
O(3)−Mn(2)−O(5)	100.17(9)	O(3)−Mn(2)−O(7)	171.06(8)
O(5)−Mn(2)−O(7)	86.49(8)		
Hydrogen Bonds			
O(7)···O(3′)	2.938(3)	O(7)−H(O7)···O(3′)	161(3)

[a] Symmetry: ′ = 1 − *x*, 1 − *y*, 1 − *z*.

manganese(II) acetate tetrahydrate under anaerobic conditions leads to complexes characterized by the same empirical composition: $Mn_2L(CH_3CO_2)_2(CH_3OH)$. This composition which is analogous to that obtained from the reaction of H_2L^1 and H_2L^2 with copper acetate,[8b] i.e. $Cu_2L(CH_3CO_2)_2$, clearly shows that H_2L^1, H_2L^2, and H_3L^3 are prone to act as dinucleating ligands provided the resulting structure is stabilized by bridging exogenous anions of the carboxylate type. The presence of one molecule of methanol per dinuclear unit in all three complexes is indicative of its involvement as a ligand to manganese and is probably related to the higher coordinative requirement of manganese compared to copper.

Molecular Structure of $[Mn_2L^1(CH_3CO_2)_2(CH_3OH)]_2$ (1). The complex molecule shown in Figure 2 is located on a crystallographic inversion center in the unit cell. Each molecule includes four manganese ions, two L^1 ligands coordinated to Mn(1) through N(1), N(2), and O(2) and to Mn(2) through O(1), O(1′), and O(2), four acetate ligands bridging Mn(1) to Mn(2), and two methanol molecules, the O(7) oxygen donors from the methanol ligands supplementing the Mn(2) coordination spheres. The L^1 catecholate oxygen atoms O(1) and O(2) are thus simultaneously bridging (Mn(1)−O(2)−Mn(2) and Mn(2)−O(1)−Mn(2′)) and chelating (Mn(2)). The average C−O and C−C bond lengths of the catecholate ring of L^1 are 1.331 and 1.397 Å, respectively, supporting the Mn(II)−catecholate formulation,[17] together with the Mn−N and Mn−O bond lengths (Table 3).

Inside each dinuclear unit, Mn(1) and Mn(2), bridged by two acetate and the O(2) catecholate oxygen atoms, are separated by a distance of 3.4135(6) Å while the Mn(2)···Mn(2′) distance resulting from the O(1) and O(1′) catecholate oxygen bridges is 3.2970(8) Å. The Mn(1)−O(2)−Mn(2) angle is larger than Mn(2)−O(1)−Mn(2′) (107.93(8)° *vs* 101.45(8)°) due to the presence of two acetate bridges which push the Mn atoms apart in comparison to the phenolato single-atom bridges. The resulting arrangement of the four manganese atoms whose center of symmetry is located at the center of the Mn(2)−O(1)−Mn(2′)−O(1′) parallelogram is chainlike with a Mn(1)···Mn(2)···Mn(2′) angle of 139.1°. It is worth noticing that the cohesion of this bis-dinuclear arrangement is strengthened by O(7)−H(O7)···O(3′) hydrogen bonds linking the methanolic oxygen atom of each dinuclear unit to one of the acetato oxygen atoms of the related dinuclear unit in the molecule (Figure 2 and Table 3). There are two bis-dinuclear complex molecules per unit cell and the crystal packing results from van der Waals interactions. This type of bis-dinuclear linear arrrangement of manganese ions is reminiscent of that afforded by the *N*,*N*,*N*′,*N*′-tetrakis(2-pyridylmethyl)-2-hydroxypropane-1,3-diamine ligand.[6a−d]

The symmetry of the N_2O_3 donor set around the outer Mn(1) is close to a trigonal bipyramid. The N(1) imine nitrogen atom of L^1 and O(4) and O(6) acetate oxygen atoms occupy the basal plane with metal−ligand distances ranging from 2.045(3) to 2.191(3) Å while the N(2) pyridine nitrogen and O(2) phenolate oxygen atoms of L^1, situated at the apices of the bipyramid (O(2)−Mn(1)−N(2) angle ∼ 155°), are separated from the manganese atom by distances of 2.216(3) and 2.056(2) Å, respectively. The O_6 ligand environment of the inner Mn(2) can be described as a rhombically distorted octahedron, the basal plane of which includes the O(1), O(2), and O(1′) catecholate and O(5) acetate oxygen atoms with metal−ligand distances ranging from 2.096(2) to 2.165(2) Å. The O(3) acetate and O(7) methanol oxygen donors separated from Mn(2) by distances of 2.220(2) and 2.354(2) Å, respectively, are situated at the apices of this elongated octahedron.

The molecular crystal structure of the related $[Cu_2(L^2)_2(CH_3CO_2)_2]_2{\cdot}H_2O$ complex involving L^2 has been previously described,[8] and it is interesting to compare the main features of the two structures. The pyridine ring and the imine nitrogen of the ligand are linked by a methylene bridge in L^1 and an ethylene bridge in L^2, thus affording a five-membered *−Mn(1)−N(1)−C(8)−C(9)−N(2)−* ring in the manganese compound and a six-membered *−Cu(1)−N(1)−C(8)−C(9)−C(10)−N(2)−* ring in the copper complex. As the adjacent six-membered *−Mn(1)−N(1)−C(7)−C(5)−C(6)−O(2)−* ring is similar to the *−Cu(1)−N(1)−C(7)−C(5)−C(6)−O(2)−* one, the strain imposed by the five-membered ring results in a significant change in the N(2)−M−O(2) angle which departs significantly from 180° in the Mn complex (154.99(9)°) while it is 177.1(2)° in the Cu compound. The distortion of the coordination polyhedron around Mn(1) and Cu(1) can be quantified using the approach of Muetterties and Guggenberger.[18] In this method, the dihedral angles between adjacent faces (known as the shape-determining angles e_1, e_2, and e_3) are calculated in order to describe an intermediate geometry. The key shape-determining angle, e_3, is equal to 0° for an ideal square pyramid (SP) and 53.1° for an ideal trigonal bipyramid (TBP). e_3 is equal to 26.38° for the manganese complex and 42.78° for the copper analog, confirming that the departure from the ideal trigonal bipyramid is larger for the Mn(1) than for the Cu(1) coordination polyhedron.[19] The other important difference between these two bis-dinuclear complex molecules concerns the coordination geometry around the inner metal ions and results from the presence of two coordinated methanol molecules in the manganese compound. While the Cu(2) ligand environment is square pyramidal with the apical position occupied by the O(6) acetate oxygen atom, the Mn(2) ligand environment is distorted

(17) (a) Larsen, S. K.; Pierpont, C. G.; DeMunno, G.; Dolcetti, G. *Inorg. Chem.* **1986**, *25*, 4828. (b) Hatrl, F.; Antonin, A., Jr.; De Learie, L. A.; Pierpont, C. G. *Inorg. Chem.* **1990**, *29*, 1073.

(18) Muetterties, E. L.; Guggenberger, L. J. *J. Am. Chem. Soc.* **1974**, *96*, 1748.

(19) Supporting Information.

octahedral with the second apical position occupied by the O(7) methanolic oxygen atom.

IR Spectroscopy. Table S6[19] lists some pertinent IR frequencies for the isolated ligands and their manganese complexes together with our proposed assignments. H_2L^1 and H_2L^2 exhibit a strong and very broad absorption (3100−2500 cm^{-1}) characteristic of hydrogen-bonded phenolic and imine or pyridine functions.[20] At variance with H_2L^1 and H_2L^2, H_3L^3 exhibits resolved absorptions in the high-frequency range: The 2750−2350 and 2000−1750 weak and broad absorptions are typical of NH···N intermolecularly hydrogen-bonded imidazole rings.[21] The C═N imine stretching mode is observed at 1625 cm^{-1} for the three ligands, clearly indicating formation of the Schiff bases. All three ligands exhibit four IR absorptions in the 1450−1200 cm^{-1} range which have been assigned to the ν_{CO} catechol stretches.[22] Absorptions typical of the pyridine ring (around 750, 635, and 405 cm^{-1}) are observed in the spectra of H_2L^1 and H_2L^2 while the characteristic imidazole ring wavenumbers (around 1310, 830, 740, and 625 cm^{-1}) are present in the spectrum of H_3L^3.

The involvement of the imine nitrogen atoms in the coordination to the metal centers of complexes **1**−**3** is evidenced by the downward shift of the corresponding $\nu_{C=N}$ frequencies (Table S6[19]). Similarly, deprotonation of the catechol functions and involvment of the catecholate oxygen atoms in the coordination to manganese is indicated by the lack of broad high-frequency features assigned to O−H···N or NH···N hydrogen bonds in the uncoordinated ligands and shifts in the characteristic 1420−1210 cm^{-1} catechol C−O absorptions. The ν_{NH} absorption at 3322 cm^{-1} for the chelated L^3 ligand clearly indicates the absence of NH···N bonds consecutive to coordination of the imine nitrogen atom of the imidazole ring in its protonated form (**3**). The ∼635 cm^{-1} $\nu_{C=C}$ pyridine absorption experiences an upward shift of 20 cm^{-1} as usually observed upon coordination.[23]

The asymmetric and symmetric COO^- absorptions observed for the acetate anions of complexes **1**−**3** are close to 1585 and 1435 cm^{-1}, respectively, affording a Δ ($=\nu_{as}(CO_2^-) - \nu_s(CO_2^-)$) value of ∼150 cm^{-1}, characteristic of bridging acetates.[24] We tentatively assign the low-frequency absorptions observed in the IR spectra of complexes **1**−**3** and lacking in the ligand spectra to Mn−L vibration modes, some of them being probably coupled to ligand vibrations.[23,25]

Finally, on the basis of the elemental data which afford the general formulation $Mn_2L(CH_3CO_2)_2(CH_3OH)$ and in consideration of the molecular structure of **1** and the common IR features obtained for **1**−**3**, we assume a similar $(Mn_2L(CH_3CO_2)_2(CH_3OH))_2$ tetranuclear structure for complexes **1**−**3**.

EPR Spectroscopy and Magnetic Susceptibility Studies. The X-band powder spectra of complexes **1**−**3** exhibit a temperature independent (300−80 K) and featureless broad resonance with a $g \sim 2$ value. The broadness of these isotropic EPR absorptions is consistent with the presence of magnetically interacting manganese(II) ions in the solid state.[26] The X-band frozen solution EPR spectra obtained from DMF/toluene or $C_2H_4Cl_2$/toluene glasses at 90 K are similar to the powder spectra, indicating that the interactions operating in the solid state are retained in solution for all three complexes.

Table 4. Effective Magnetic Moment (μ_B/Mn) at Selected Temperatures for Complexes **1**−**3**

		temp (K)				
no.	complex	300	100	50	20	2
1	$[Mn_2L^1(CH_3CO_2)_2(CH_3OH)]_2$	5.46	4.55	3.55	2.27	0.74
2	$(Mn_2L^2(CH_3CO_2)_2(CH_3OH))_2$	5.55	4.96	4.19	2.80	0.84
3	$(Mn_2HL^3(CH_3CO_2)_2(CH_3OH))_2$	5.64	4.92	4.03	2.64	0.80

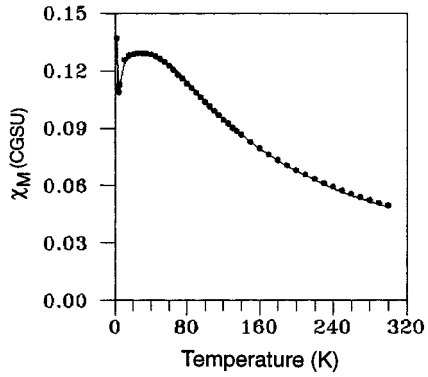

Figure 3. Variable-temperature magnetic susceptibility data for $[Mn_2L^1(CH_3CO_2)_2(CH_3OH)]_2$ (**1**). The solid lines result from a least-squares fit of the data to the theoretical magnetic susceptibility calculated as mentioned in the text.

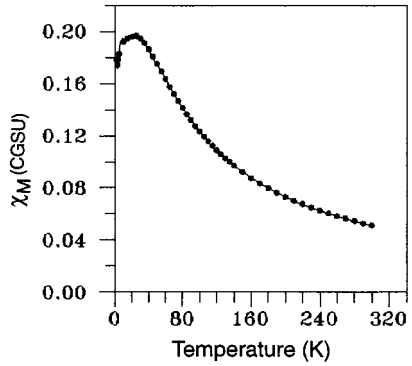

Figure 4. Variable-temperature magnetic susceptibility data for $(Mn_2L^2(CH_3CO_2)_2(CH_3OH))_2$ (**2**). The solid lines result from a least-squares fit of the data to the theoretical magnetic susceptibility calculated as mentioned in the text.

The effective magnetic moment per manganese at selected temperatures is reported in Table 4 for complexes **1**−**3**, and the detailed data resulting from the 300−2 K magnetic susceptibility measurements are available.[19] The temperature dependence of the magnetic susceptibility and effective magnetic moment per manganese of the Mn(II) bis-dinuclear complexes **1**−**3** are shown in Figures 3−5, respectively. μ_{eff}/Mn is lower than the spin only value at 300 K and decreases from 5.46, 5.55, and 5.64 μ_B to 0.74, 0.84, and 0.80 μ_B at 2 K for **1**, **2**, and **3**, respectively, indicating overall antiferromagnetic coupling of the $S = {}^5/_2$ spin systems of the manganese(II) ions in all three complexes.

(20) (a) Freeman, H. H. *J. Am. Chem. Soc.* **1961**, *83*, 2900. (b) Gramstad, T. *Acta Chem. Scand.* **1962**, *16*, 807.
(21) Zimmerman, H. *Z. Elektrochem.* **1959**, *63*, 608.
(22) Bellamy, L. J. *The Infrared Spectra of Complex Molecules*, 3rd ed.; Chapman and Hall: New York, 1975; Vol. I.
(23) Nakamoto, K. *Infrared and Raman Spectra of Inorganic and Coordination Compounds*, 4th ed.; Wiley: New York, 1986.
(24) Deacon, G. B.; Phillips, R. J. *Coord. Chem. Rev.* **1980**, *33*, 227.
(25) Ferraro, J. R. *Low Frequency vibrations of inorganic and coordination compounds*; Plenum Press: New York, 1971.
(26) (a) Dowsing, R. D.; Gibson, J. F.; Goodgame, D. M.; Goodgame, M.; Hayward, P. J. *Nature (London)* **1968**, *219*, 1037. (b) Dowsing, R. D.; Gibson, J. F.; Goodgame, M.; Hayward, P. J. *J. Chem. Soc. A* **1969**, 187. (c) Dowsing, R. D.; Gibson, J. F.; Goodgame, D. M.; Goodgame, M.; Hayward, P. J. *J. Chem. Soc. A* **1969**, 1242. (d) Abragam, A.; Bleaney, B. *Résonance Paramagnétique Electronique des Ions de Transition;* Presses Universitaires de France: Paris, 1971. (e) Goodman, B. A.; Raynor, J. B. *Adv. Inorg. Chem. Radiochem.* **1970**, *13*, 205. (f) Mabad, B.; Cassoux, P.; Tuchagues, J. P.; Hendrickson, D. N. *Inorg. Chem.* **1986**, *25*, 1420.

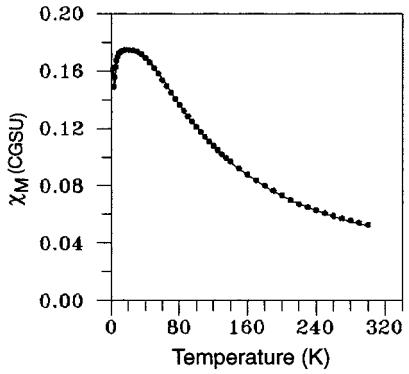

Figure 5. Variable-temperature magnetic susceptibility data for $(Mn_2HL^3(CH_3CO_2)_2(CH_3OH))_2$ (**3**). The solid lines result from a least-squares fit of the data to the theoretical magnetic susceptibility calculated as mentioned in the text.

The X-ray molecular structure of **1** shows the absence of hydrogen-bond network or ring stacking interaction between neighboring tetranuclear molecules. The interaction pathway between inner and outer manganese(II) ions involves one monoatomic (catecholate oxygen) and two acetate bridges affording a Mn(1)···Mn(2) separation of 3.4135(6) Å while two monoatomic (catecholate oxygens) and two triatomic (hydrogen bonds) bridges mediate the interaction between inner manganese ions with a Mn(2)···Mn(2′) separation of 3.2970(8) Å. It is thus clear that among the six possible superexchange interactions between the four paramagnetic centers of a tetranuclear complex, only the Mn(1) ↔ Mn(2), Mn(1′) ↔ Mn(2′), and Mn(2) ↔ Mn(2′) ones need be considered in the present case. The superexchange pathway between the symmetry related Mn(2) and Mn(2′) ions characterized by the same axially elongated cubic ligand field results from overlap between the O(1) and O(1′) ligand based orbitals and $d_{x^2-y^2}$ magnetic orbitals. It has already been shown that this type of superexchange pathway mediates both ferro- and antiferromagnetic contributions to the overall magnetic interaction, and the resulting exchange integral J_{ij} ($-2J_{ij}S_iS_j$) may be either positive or negative.[27] On the other hand, the superexchange pathway between Mn(1) and Mn(2) (Mn(1′) and Mn(2′)) essentially results from overlap of the Mn(1) (Mn(1′)) d_{z^2} (distorted TBP ligand environment) and Mn(2) (Mn(2′)) $d_{x^2-y^2}$ magnetic orbitals with the O(2) (O(2′)) ligand-based orbitals. In the following, the exchange integral characterizing the Mn(2) ↔ Mn(2′) interaction between inner metal ions is noted J_1 while the exchange integral characterizing the Mn(1) ↔ Mn(2) (=Mn(1′) ↔ Mn(2′)) interaction between inner and outer metal ions is noted J_2 ($=J_4$).

The magnetic susceptibility of **1** has been analyzed by employing the rigorous method based on exact diagonalization of the effective spin hamiltonian for a $^5/_2-^5/_2-^5/_2-^5/_2$ spin system in the 1296 uncoupled spin states basis set.[28] Owing to the results previously gained from the extensive study of the $^5/_2-^5/_2-^5/_2-^5/_2$ spin system, and in order to avoid overparametrization, we have set the single ion axial zero-field splitting, D, to zero and considered a unique isotropic g factor in order to evaluate the order of magnitude for the main parameters, J_1 and J_2 ($=J_4$). Prior to fitting the experimental data, a detailed scanning of the $-25 \le J_1 \le 5$ cm^{-1} and $-15 \le J_2$ ($=J_4$) ≤ 3 cm^{-1} ranges has been carried out, locating two minima of the error function Er (NP = number of data points),

$$\mathrm{Er} = \sum_{i=1}^{\mathrm{NP}} [\chi_{\mathrm{M}}(\mathrm{obsd})_i - \chi_{\mathrm{M}}(\mathrm{calcd})_i]^2$$

namely, $J_1 \sim -0.5$ cm^{-1}, J_2 ($=J_4$) ~ -4.5 cm^{-1}, and Er $= 1.2 \times 10^{-5}$ and $J_1 \sim 0.5$ cm^{-1}, J_2 ($=J_4$) ~ -5 cm^{-1}, and Er $= 2 \times 10^{-5}$. Considering this result, and the presence of a paramagnetic tail at very low temperature, we fitted the experimental data with 4 independently varying parameters, J_1, $J_2 = J_4$, g_i, and Par (%) (J_3, J_5, J_6, and D_i ($i = 1-4$) set to zero). Good fits were obtained for the sets of parameter values $J_1 = -0.49$ cm^{-1}, J_2 ($=J_4$) $= -5.06$ cm^{-1}, $g = 1.982$, Par $=$ 1.5%, and Er $= 1.1 \times 10^{-5}$ (Figure 3) and $J_1 = 0.59$ cm^{-1}, J_2 ($=J_4$) $= -5.11$ cm^{-1}, $g = 1.963$, Par $= 1.5\%$, and Er $= 2.5 \times 10^{-5}$ (not shown), indicating that $|J_1|$ is ~10% of $|J_2|$ and that its sign cannot be determined unambiguously. Finally, taking into account the minute J_1 value and the ambiguity in its sign, we also fitted the experimental data with J_1 set to zero (3 independently varying parameters, $J_2 = J_4$, g_i, and Par (%)). The ambiguity in the sign of the interdinuclear magnetic interaction was confirmed by the similar quality of the fit obtained (not shown) with the following parameter values: J_2 ($=J_4$) $= -5.01$ cm^{-1}, $g = 1.963$, Par $= 1.5\%$, Er $= 6 \times 10^{-5}$.

As previously discussed on the basis on their similar formulation and IR and EPR features, complexes **2** and **3** have most probably a bis-dinuclear structural arrangement very similar to that evidenced by the X-ray single-crystal study of **1**. This hypothesis being also supported by their similar magnetic behavior, we have analyzed the thermal variation of the magnetic susceptibility of **2** and **3** by employing the above-mentioned rigorous method[28] and the same assumptions as for complex **1**: 3 independently varying parameters ($J_2 = J_4$, g_i, and Par (%)), and J_1, J_3, J_5, J_6 and D_i set to zero. The least-squares refinement of the theoretical magnetic susceptibility calculated from this model to the experimental data afforded good fits for the parameter values: J_2 ($=J_4$) $= -3.36$ cm^{-1}, $g = 1.966$, Par $= 1.7\%$, Er $= 5 \times 10^{-5}$ (**2**, Figure 4); J_2 ($=J_4$) $= -3.84$ cm^{-1}, $g = 1.990$, Par $= 1.7\%$, Er $= 2 \times 10^{-5}$ (**3**, Figure 5). The similar exchange parameters obtained for complexes **1**−**3** affords additional evidence of their structural analogy. Moreover, the fact that equally good fits are obtained for **1**−**3** with the same $J_1 = 0$ assumption agrees well with the observation that the differences in the L^1-L^3 ligand structure cannot induce significant changes in the Mn(2) (Mn(2')) coordination geometry and, consequently, in the Mn(2)···Mn(2′) bridge. By contrast, in agreement with the differences in J_2 ($=J_4$) values observed for complexes **1**−**3**, the distortion of the Mn(1) (Mn(1′)) TBP ligand environment toward SP, and consequently the geometry of the Mn(1)···Mn(2) and Mn(1′)···Mn(2′) bridges, is dependent upon the differences in L^1-L^3 ligand structure.

Electrochemical and Dioxygen Oxidation Studies. According to their solubility, H_2L^1, H_2L^2, H_3L^3, and complexes **1**−**3** have been studied by linear (LV) and cyclic voltammetry (CV) in DMF and/or DMSO with tetrabutylammonium tetrafluoroborate (TBATFB) or tetrabutylammonium perchlorate (TBAP) as supporting electrolyte.

Caution: Perchlorate salts are potential explosives and should be handled in small quantities and with much care!

The CV profiles of H_2L^1 and H_2L^2 exhibit two successive one-electron oxidation processes around 0.7 and 1.3 V corresponding to quasi-reversible conversion of catechol to semiquinone and quinone, respectively,[8] while the CV profile of H_3L^3 exhibits irreversible oxidation processes at 0.67 and 0.92 V. At variance with the case of H_2L^1 and H_2L^2, a drop in diffusion current is observed above 0.7 V in the LV profile of H_3L^3,

(27) Lambert, S. L.; Hendrickson, D. N. *Inorg. Chem.* **1979**, *18*, 2683.
(28) (a) Aussoleil, J.; Cassoux, P.; de Loth, P.; Tuchagues, J. P. *Inorg. Chem.* **1989**, *28*, 3051. (b) Bousseksou, A.; Tuchagues, J.-P. Submitted for publication.

Table 5. Electrochemical Parameters Obtained for Complexes **1**−**3**

complex	solvent/ electrolyte	linear voltammetry: scan rate, 5 mV/s; rotation speed 1000 rpm		cyclic voltammetry: scan rate 100 mV/s	
		$E_{1/2}$ (mV)[a]	I_D (μA)	Ep_a (mV)[a]	I_{p_a} (μA)
1	DMF/TBATFB	110	7.3	180	3.3
		360	6.3	410	2.6
1	DMF/TBAP			100	1.0
				420	5.9
1	DMSO/TBATFB			100	1.0
1	DMSO/TBAP	30	5.0	90	3.0
				390	3.1
2	DMF/TBATFB	120	6.3	200	3.7
				530	4.4
2	DMF/TBAP	140	5.3	210	2.6
				520	2.9
3	DMF/TBATFB	100	5.2	160	3.6
3	DMF/TBAP	110	6.7	170	3.9
3	DMSO/TBATFB	37	4.1	100	2.5
3	DMSO/TBAP	25	5.0	80	2.8
				350	2.6

[a] *Vs* SCE.

indicating that an adsorption or a passivation phenomenon is occurring at the working electrode.

Depending upon the solvent and supporting electrolyte, complexes **1**−**3** undergo one or two irreversible electrochemical oxidations regardless of the CV scan rate and nature of the working electrode. The results obtained with a platinum electrode and a scan rate of 0.1 V s^{-1} are reported in Table 5, showing that the first oxidation potential is in the 0−0.2 V range *vs* SCE while the second oxidation potential is in the 0.4−0.5 V range *vs* SCE, when observable. Since the ligand oxidation does not occur up to 0.7 V, both anodic peaks can be attributed to successive oxidations of Mn(II) ions of the bis-dinuclear complexes, in agreement with similar results obtained for Mn(II) Schiff base complexes.[26f] As confirmed by LV, both oxidations of **1** and the first oxidation of **2** and **3** are two-electron processes. As for H_3L^3, a drop in diffusion current is observed after the first oxidation (∼0.2 V) in the LV profiles of **2** and **3**, indicating that an adsorption or a passivation phenomenon is occurring at the working electrode and precluding assessment of the number of electrons involved in the second oxidation process. However, on the basis of a comparison of anodic peak currents in the CV experiments, it is likely that both oxidations are also two-electron processes in **2** and **3**.

Owing to the presence of the pyridine or imidazole and imine nitrogen donors, the Mn(II) state of both outer manganese ions (N_2O_3 ligand environment) should be stabilized toward oxidation compared to the Mn(II) state of both inner manganese ions (O_6 ligand environment).[29] This rationale suggests that the inner Mn(II) ions are oxidized at a potential lower than that of the outer Mn(II) ions. The irreversibility of the electrochemical oxidation, indicative of the simultaneous occurence of a chemical reaction, is in agreement with this hypothesis as oxidation of the inner Mn(II) centers may be accompanied by a reorganization of their coordination sphere large enough to induce the release of isolated dinuclear units. On the other hand, oxidation of the outer Mn(II) ions prior to the inner ones would not result in such a dramatic effect, considering that the pentacoordinated metal centers are both chelated by the N(2), N(1), and O(2) donors of the polydentate ligand and bridged by its O(2) donor to the inner manganese ion. Furthermore, dioxygen oxidation studies reported in the following paragraph support this analysis.

(29) (a) Coleman, W. M.; Taylor, L. T. *Coord. Chem. Rev.* **1980**, *32*, 1. (b) Connors, H.; McAuliffe, C. A.; Tames, J. *Rev. Inorg. Chem.* **1981**, *3*, 199.

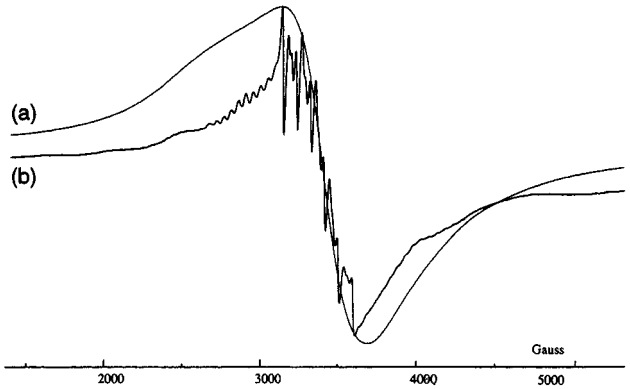

Figure 6. X-band DMF/toluene glass EPR spectra of $(Mn_2HL^3(CH_3CO_2)_2(CH_3OH))_2$ (**3**) at 90 K before (a) and after (b) reaction with O_2 (O_2:**3** ratio ∼ 1:2; microwave power 20 mW; microwave frequency 9.4225 GHz (a), 9.4264 GHz (b); 10-G modulation amplitude).

Yellow DMF/toluene and $C_2H_4Cl_2$/toluene solutions of complexes **1**−**3** prepared under strictly anaerobic conditions were allowed to react with controlled amounts of dioxygen. The solutions slowly turned brown (**1**, **2**) or greenish-brown (**3**), finally affording small amounts of brown (**1**, **2**) or bronze (**3**) precipitates after a few weeks. These O_2 oxidation reactions were monitored with EPR spectroscopy. Comparison of the EPR spectra of frozen solutions (90 K) of the three complexes recorded before and after reaction with small amounts of O_2 (O_2:complex ratios lower than ∼1:1.5) indicates that the first step of the reaction of complexes **1**−**3** with dioxygen results in the release of dinuclear Mn(II) species characterized by several fine structure absorptions exhibiting the typical 11-line hyperfine pattern of ^{55}Mn pairs.[26f] However, this first intermediate is not stable and EPR spectra recorded either after longer reaction times or for reaction mixtures containing larger amounts of dioxygen show not only the typical dinuclear absorptions but also a $g \sim 2$ centered six-line hyperfine pattern indicative of the presence of mononuclear Mn(II) species. The six-line hyperfine pattern increases at the expense of the absorptions characteristic of the dinuclear species, as a function of time. For long reaction times (weeks) or O_2:complex ratios higher than ∼1:1.5 the absorptions characteristic of the dinuclear species have vanished and the $g \sim 2$ centered six-line pattern has decreased while an EPR silent brown precipitate has deposited at the bottom of the EPR tube. Typical DMF/toluene glass EPR spectra of complex **3** before and after reaction with a O_2:**3** ratio of ∼1:2 are shown in Figure 6. All attempts at characterizing the final EPR silent brown precipitates were unsuccessful, indicating the presence of a mixture of Mn(III) species. Although it is not possible to suggest any satisfactory hypothesis for the oxidation reaction pathway between complexes **1**−**3** and O_2, monitoring of these reactions with EPR spectroscopy evidences similar reaction pathways for all three complexes including the following: (i) splitting of the bis-dinuclear complexes into dinuclear species; (ii) splitting of the dinuclear species into mononuclear species.

Thus, regardless of the chemical or electrochemical nature of the oxidation, the investigated bis-dinuclear complexes are broken down during the oxidation process. Although we have already observed the same type of behavior while studying tetranuclear[5a] and dodecanuclear[30] Mn^{II} complexes, we are not aware of literature reports including similar observations concerning the oxidation of tetranuclear or higher nuclearity Mn^{II} complexes. On the other hand, several oxidation studies

(30) Luneau, D.; Savariault, J.-M.; Tuchagues, J.-P. *Inorg. Chem.* **1988**, *27*, 3912.

carried out on dinuclear Mn^{II} complexes have shown that tetranuclear complexes with higher manganese oxidation states may be generated through establishment of oxo or peroxo bridges between precursor dinuclear units and rearrangement of the manganese coordination spheres.[7d,31] More studies are needed in order to determine if this is a general trend among Mn^{II} complexes, and the oxidation study of several new series of tetranuclear Mn^{II} complexes undertaken in our groups will be published shortly.

Conclusion

The chainlike bis-dinuclear Mn(II) complex **1** described in this work involves an unprecedented arrangement of pentacoordinated (N_2O_3) and hexacoordinated (O_6) manganese ions as the outer and inner pairs of metal centers, respectively. The different Mn···Mn distances result from significant differences in bridging moieties, two catecholato bridges for the shortest distance between inner manganese ions and one catecholato and two acetato bridges for the longer distances between inner and outer manganese ions. The later bridges lead to antiferromagnetic exchange while the former results in magnetic interactions weak to the point that the sign of the exchange integral (J_1) cannot be unambiguously determined. Analytical results, IR and EPR spectroscopy, and magnetic properties suggest a similar structure for complexes **1**−**3**. EPR spectroscopy indicates that the solid-state structure of complexes **1**−**3** is retained in aprotic solvents. As shown by EPR, O_2 oxidation leads to the release of the constitutive Mn(II) dinuclear units, prior to formation of mononuclear Mn(II) and finally Mn(III) species. Observation of two irreversible two-electron oxidation waves in the CV profiles of **1**−**3** is consistent with a similar splitting of the bis-dinuclear complex molecules induced by electrochemical oxidation. Finally, catecholimine ligands such as H_2L^1, H_2L^2, and H_3L^3 are particularly well suited to generate bis-dinuclear manganese structures characterized by oxygen-rich donor environments and the presence of imidazole rings (H_3L^3) close to manganese ions, both characteristics being of interest with regard to the modeling of the manganese cluster in the OEC.[9,32] However, regardless of the chemical or electrochemical nature of the oxidation the investigated bis-dinuclear complexes are broken down during the oxidation process. These studies suggest that complexes resulting from the reaction of manganese with the fully oxidized form of such electroactive ligands may afford interesting new higher oxidation-state polynuclear Mn species. We are presently investigating such possibilities.

Acknowledgment. R.Y., R.C., and S.P. acknowledge financial support from the CSIR, New Delhi, India. We are indebted to the reviewers for their particularly constructive comments.

Supporting Information Available: A listing of complete crystal data and experimental details, listings of final fractional atomic coordinates with their estimated standard deviations, components of the anisotropic temperature factors, hydrogen atomic positional and thermal parameters, bond lengths and angles, and least-squares planes and deviations of atoms therefrom for complex **1**, and listings of detailed data resulting from the IR and magnetic susceptibility measurements for complexes **1**−**3** in the 300−2 K temperature range (13 pages). Ordering information is given on any current masthead page.

IC9703538

(31) Mabad, B.; Tuchagues, J.-P. Hwang, Y. T.; Hendrickson, D. N. *J. Am. Chem. Soc.* **1985**, *107*, 2801.
(32) Penner-Hahn, J. E.; Fronko, R. M.; Pecoraro, V. L.; Yocum, C. F.; Betts, S. D.; Bowlby, N. R. *J. Am. Chem. Soc.* **1990**, *112*, 2549.